Solid-State NMR Spin Diffusion for Measurement of Membrane-Bound Peptide Structure: Gramicidin A[†]

Greg J. Gallagher,[‡] Mei Hong,[§] and Lynmarie K. Thompson*,[‡]

Department of Chemistry, University of Massachusetts, Amherst, Massachusetts 01003-9336, and Department of Chemistry, Iowa State University, Ames, Iowa 50011-3111

Received September 7, 2003; Revised Manuscript Received March 30, 2004

ABSTRACT: A recently developed solid-state NMR method for measurement of depths in membrane systems is applied to gramicidin A, a membrane-bound peptide of known structure, to investigate the potential of this method. ^{15}N-detected, ^{1}H spin diffusion experiments demonstrate the resolution of the technique by measuring the 4−5 Å depth differences between three ^{15}N-labeled backbone sites (Trp13, Val7, Gly2) in gramicidin A. We also show that ^{13}C-detected, ^{1}H spin diffusion experiments on *unlabeled* gramicidin A are sufficient to discriminate between the end-to-end dimer and double-helix structures of gramicidin A. Thus, spin diffusion solid-state NMR experiments can provide a simple approach, which does not require labeled samples, for testing structural models of membrane-bound peptides.

Despite advances in crystallization methods for membrane proteins (*1*−*3*) and advances in solution NMR[1] methods for large complexes (*4*), the challenges of understanding structure and mechanism of membrane proteins and peptides typically requires application of a variety of techniques. EPR studies employing spin labels attached to cysteine residues introduced via site-directed mutagenesis can give secondary structure information by measuring periodic signal properties, membrane depth information by measuring differential accessibility to hydrophobic and hydrophilic relaxation agents, and distance information by measuring spin−spin interactions (*5*−*7*). Fluorescence studies use fluorophores in a similar manner to measure depths and distances (*8*−*10*). Solid-state NMR measurements of distances and angles provide a variety of means to measure secondary and tertiary structure of membrane peptides and proteins (*11*, *12*). These can provide complementary approaches for probing membrane protein structure and mechanism, since the NMR methods are often less sensitive than EPR and fluorescence methods but also do not require the introduction of spin or fluorescent labels.

Proton spin diffusion with X-nucleus detection is a solid-state NMR technique that has been recently developed for measuring depths in membranes (*13*, *14*). This technique, which was originally used to characterize domain sizes in polymer blends (*15*), exploits the large difference in the relaxation properties of protons within the sample. In frozen membrane vesicle samples, protons of the rigid gel-phase membrane and membrane proteins have very short T_2 relaxation times and the protons of the mobile, surface-associated water have longer T_2 relaxation times. The experiment (pulse sequence shown in Figure 1) begins with proton excitation immediately followed by a T_2 filter (τ_d), which filters out the rigid proton magnetization of the protein and lipids. The remaining mobile water proton magnetization undergoes spin diffusion into the membrane during t_m, and the magnetization is then transferred via cross polarization to ^{31}P, ^{13}C, or ^{15}N nuclei in the lipid and protein for detection. The spin diffusion time needed to build the signal intensity is correlated with the depth of the site. The crucial aspect of this experiment is that the water is mobile enough to have a T_2 of 300 μs yet is still immobile enough ($\Delta\nu_{1/2} = 300$ Hz) for efficient proton−proton magnetization transfer (*14*).

Spin diffusion depth measurements performed on uniformly ^{15}N-labeled membrane-bound colicin E1 (*14*) demonstrated that at least 70% of its residues are located near the surface of the membrane, consistent with both proposed models of the membrane-bound structure of this protein (*16*). A variation of the spin diffusion technique applicable to unfrozen samples has been developed for which the mobile lipid methyl protons (headgroup and tail) serve as the sources of magnetization (*13*). Results of this technique applied to membrane-bound colicin Ia discriminate between the two structural models by indicating that some of the protein is membrane-inserted (*13*). Thus, spin diffusion has provided qualitative depth measurements providing insight into structures of membrane proteins.

This paper examines the utility of spin diffusion for quantitative depth measurements to characterize structure in frozen samples of membrane-bound peptides. Gramicidin A, a 15 residue peptide with a known structure in DMPC bilayers (*17*), was chosen in order to demonstrate the potential resolution of spin diffusion depth measurements. In lipid bilayers, gramicidin A adopts a β-helix structure and forms an end-to-end dimer that spans the membrane. Alternative structures of gramicidin A have been proposed such as a double helix, which is observed in crystals from

[†] This research was supported by U.S. Public Health Service Grant GM47601 (to L.K.T.).

* To whom correspondence should be addressed. E-mail: thompson@chem.umass.edu. Phone: (413) 545−0827. Fax: (413) 545−4490.

[‡] University of Massachusetts.

[§] Iowa State University.

[1] Abbreviations: CPMAS, cross-polarization and magic angle spinning; DMPC, 1,2-dimyristoyl-sn-glycero-3-phosphocholine; DPPC, 1,2-palmitoyl-sn-glycero-3-phosphocholine; EPR, electron paramagnetic resonance; gA, gramicidin A; NMR, nuclear magnetic resonance.

10.1021/bi0356101 CCC: $27.50
Published on Web 05/27/2004

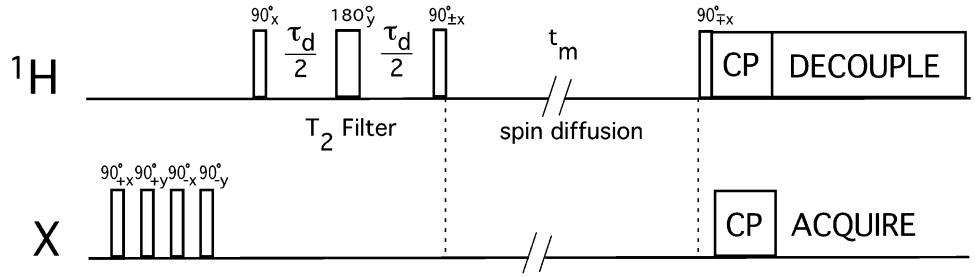

FIGURE 1: Spin diffusion pulse sequence (*14*). Any X magnetization is destroyed by several 90° pulses with a 2 μs interval, followed by a dipolar dephasing period. After ^{1}H excitation, a T_2 filter ($\tau_d = 200$ μs) allows rigid proton magnetization to decay. Then, a 90° pulse stores the remaining magnetization of the mobile water protons on the *z*-axis for the variable spin diffusion time (t_m), which ranges from 0 to 100 ms. Finally, a cross-polarization sequence transfers the proton magnetization to the desired X nucleus for detection.

organic solvents (*18*−*21*). We have performed spin diffusion measurements on site-specifically labeled samples of gramicidin A in DMPC vesicles. The three chosen ^{15}N-labeled backbone sites (Trp13, Val7, Gly2) are separated by 4−5 Å depth differences in the end-to-end dimer structure (*22*). The spin diffusion results are consistent with the predicted depths and depth differences, which demonstrates the capabilities of this approach for quantitative depth measurements. Additionally, spin diffusion experiments on unlabeled gramicidin A are shown to be sufficient to distinguish between the double helix and the end-to-end dimer structures, making this a simple method for testing proposed structures of membrane-bound peptides.

MATERIALS AND METHODS

Preparation of Large Unilamellar Vesicles. 1,2-Dimyristoyl-sn-glycero-3-phosphocholine (DMPC) and 99% ^{13}C-carbonyl DMPC were purchased from Avanti Polar Lipids (Birmingham, AL). All DMPC lipids were checked for purity using thin-layer chromatography with a solvent mixture of chloroform/methanol/water (65:25:4, v/v). In 15 mL of distilled−deionized water in a polypropylene tube was suspended 150 mg of 40% ^{13}C-labeled lipid (60 mg of ^{13}C lipid:90 mg of unlabeled lipid). The mixture was freeze−thawed five times using liquid nitrogen and a 55 °C water bath. The suspension was placed in a thermal jacketed lipid extruder (Lipex biomembranes, Vancouver, Canada). The temperature of the extruder was kept at 37 °C in order to ensure that the lipid was well above its phase transition temperature (23 °C). The mixture was extruded through 100 nm polycarbonate pore filters (double stacked) 10 times. After completion, the solution was spun in an ultracentrifuge at 119 000*g* (45 000 rpm in a Ti70 rotor) for 2 h. The supernatant was discarded, and the pellet was packed in the NMR rotor.

Preparation of Gramicidin A in DMPC Bilayers. Unlabeled gramicidin A (formyl-Val1-Gly2-Ala3-DLeu4-Ala5-DVal6-Val7-DVal8-Trp9-DLeu10-Trp11-Leu12-Trp13-DLeu14-Trp15-ethanolamine) was purchased from Fluka (Ronkonkoma, NY). The laboratory of Dr. Timothy Cross kindly provided three different single ^{15}N-labeled gramicidin A peptide samples. Samples were prepared according to a protocol similar to that of Ketchem et al. (*23*), which results in a β-helix structure in membrane bilayers. To obtain a lipid-to-peptide ratio of 8:1, 150 mg (2.17×10^{-4} mol) of DMPC powder was combined with 50 mg (2.67×10^{-5} mol) of gramicidin A in a screw cap vial. The powder mixture was dissolved in 285 μL of benzene and 150 μL of ethanol. The vial was capped and incubated at room-temperature overnight. Solvent was then removed by air-drying, and the sample was resuspended in 40 mL of distilled deionized water. The suspension was spun in an ultracentrifuge at 119 000*g* for 2 h. The supernatant was discarded, and the entire sample (200 mg) was packed in a 7 mm solid-state MAS NMR rotor. The ^{15}N-Trp13, ^{15}N-Val7, and unlabeled gramicidin A samples were each individually combined with DMPC containing 40% ^{13}C-carbonyl DMPC. The ^{15}N-Gly2,1-^{13}C-Val3 gramicidin A sample was combined with unlabeled DMPC.

NMR Spectroscopy. All NMR experiments were done on a Bruker ASX NMR spectrometer with a proton resonance frequency of 300.126 MHz. A Bruker triple-resonance 7 mm MAS probe was used with 7 mm zirconia rotors and Kel-F endcaps. Sample spinning speeds of 5 kHz and ^{1}H 90° pulse widths of 5 μs were used for most spectra. Typical B_1 field strengths used in cross polarization were $\gamma B_1/2\pi = 50$ kHz for ^{13}C spectra and 35 kHz for ^{15}N spectra. Proton decoupling with $\gamma B_1/2\pi = 70$ kHz was applied during acquisition. The T_2 filter (τ_d) was 200 μs for all spin diffusion measurements. This was chosen by comparing proton spectra with different T_2 filter times to find the minimum time needed to remove the broad rigid proton resonance underlying the 300 Hz mobile water resonance. Spin diffusion times (t_m) ranged from 0.01 to 100 ms. The cross-polarization time in all heteronuclear experiments was 5 ms; half of this duration contributes to the actual spin diffusion time. All T_1 experiments were done using the spin diffusion pulse sequence with τ_d set to zero and measuring the decay of magnetization as a function of t_m. For the ^{15}N-labeled gramicidin samples (Figure 3), 100K scans were collected for each ^{15}N time point (~28 h each with a 1 s recycle delay), 12K scans were collected for each ^{13}C time point, and 6K scans were collected for each ^{31}P time point. For the unlabeled gramicidin sample, 20K scans were collected for each ^{13}C time point. Without spin diffusion, considerably stronger signals are observed (e.g., only 2K scans were collected for the unlabeled gramicidin spectrum in Figure 6). ^{13}C chemical shifts were referenced to TMS (the methyl carbon of a *p*-di-*tert*-butylbenzene external standard was set to 31 ppm).

To achieve low temperatures, the bearing gas was cooled using a double-dewar system. The bearing gas passed first through a copper coil immersed in cryocool fluid (Savant technologies) cooled by a CC-100II immersion cooler (NESLAB Instruments) and then through a second coil immersed in cryocool fluid cooled by dry ice. The second dewar was used because the immersion cooler alone is

Table 1: One-Dimensional Spin Diffusion Simulation Parameters

layer	thickness (Å)	diffusion coefficient (Å²/ms) step size 1 Å
source region (H_2O)	11.8 Å	≥300
interface	0 (one step)	2.50
total lipid + peptide	55 Å	37.5

insufficient to maintain the membrane samples frozen when long decoupling times and/or high spinning speeds are used. [Note that current experiments employ a simpler approach for sample cooling with an FTS forced air cooling unit (Kinetics thermal systems).] The ^{1}H line width (full width at half-maximum) of the H_2O was measured prior to all spin diffusion experiments. The experimental temperature was adjusted in order to achieve a ^{1}H line width of 300 Hz, to ensure the same magnetization transfer rate in different samples (see below). The range of sample temperatures was 240−250 K, calibrated by an external standard (tetrakis-(trimethylsilyl)silane soaked in methanol) (*24*).

NMR Data Analysis. Spectra within the same spin diffusion experiment (a series) were collected and processed with identical processing parameters. The peak heights in the spin diffusion experiment were corrected for the T_1 decay measured in a parallel experiment (which omitted the T_2 filter) on the same sample: the spin diffusion peak intensity was divided by the fractional intensity measured for the same t_m in the T_1 experiment. These values were then normalized to the peak height at the final mixing time value (100 ms) and plotted as a function of the square root of the mixing time. Error bars of ±1 standard deviation were estimated from the standard deviation of the noise level measured in a signal-free region of the spectrum, which was also normalized to the peak height at the final mixing time value. Intensities of resonances of unlabeled gramicidin A (Figures 6 and 7) were determined from spectral deconvolutions performed with XWINNMR.

Spin diffusion simulation curves were generated using a Fortran program (*14*) based on a one-dimensional lattice model in which proton−proton magnetization transfer proceeds at rate $\Omega = D/a^2$, which depends both on the diffusion rate D and the interspin spacing a, according to the diffusion equation (*13*), $\Delta M_i/\Delta t = -2\Omega M_i + \Omega M_{i+1} + \Omega M_{i-1}$. The M_i spin transfers a fraction of its magnetization equally to its neighbors in both directions along the lattice, but because the T_2 filter initially creates a nonequilibrium magnetization distribution (no magnetization inside the membrane), spin diffusion results in net transfer into the membrane until equilibrium is restored. Parameters used for the simulations (Table 1) are similar to those used previously (*14*), with the following modifications. The membrane thickness of gel phase DMPC is 55 Å, and the thickness of the water phase is calculated so that the percent water is equal to the final percentage value of the water signal (18%) after spin diffusion brings the magnetization distribution to equilibrium in all phases. The diffusion coefficient of 37.5 Å²/ms, which was chosen to obtain accurate depths of known sites (see below), is slightly smaller than the one used previously (40 Å²/ms). Using these parameter values, a family of curves was simulated for 1 Å depth increments. For each data set, the depth of the site was determined by using a MATLAB script to find the best fit curve by calculating the RMSD between the data and each of the simulated curves.

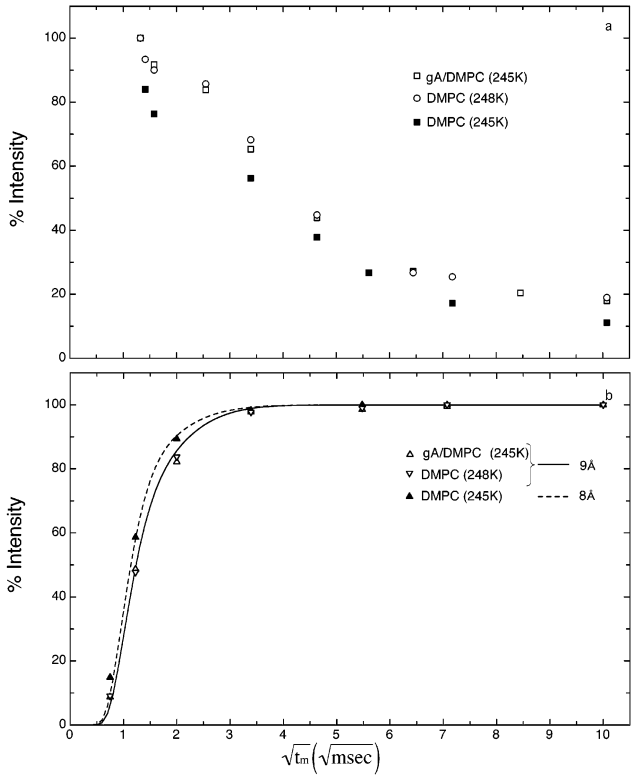

FIGURE 2: Comparison of ^{1}H and ^{13}C spin diffusion between frozen DMPC bilayer samples. The ^{1}H spin diffusion profiles (a) are similar for two samples, one of which contains gramicidin A (gA), when temperatures are chosen to achieve 300 Hz line widths (open squares at 245 K and open circles at 248 K). Under these conditions, the spin diffusion profiles (b) for the lipid carbonyl carbon are indistinguishable for these two samples (open upright and inverted triangles, respectively) and are in good agreement with a simulated spin diffusion curve for a depth of 9 Å (solid line). For the DMPC sample, a temperature of 245 K yields a different line width (250 Hz) and different spin diffusion profiles for both the ^{1}H (filled squares) and lipid carbonyl ^{13}C (filled triangles). The fact that the latter fit an 8 Å simulation curve (dashed line) demonstrates the importance of matching the line widths in order to obtain reproducible depth measurements. Error bars (see methods) are much smaller than the symbol size on the plots.

The membrane thickness and depths in DMPC bilayers were estimated on the basis of neutron diffraction studies of DPPC bilayers (*25*). The 57.4 Å bilayer thickness measured for the low-water content, gel-phase DPPC bilayer (*25*) was reduced by 1.2 Å × 2 to convert to a 55 Å thickness for the DMPC bilayers used in this study (2 carbon units shorter). This thickness was used to convert distances from the bilayer center to depths from the surface as follows. On the basis of the DPPC study, the methyl carbon (C14) is expected to be 1.7 Å from the bilayer center, at a depth of 55/2 − 1.7 ≈ 26 Å. The phosphorus and carbonyl carbons should be at similar depths from the surface in DPPC and DMPC. For each 29 Å thick DPPC monolayer, the headgroup carbons (and thus phosphorus) were ∼25 Å from the center (4 Å deep) and the carbonyl carbons were on average ∼20 Å from the center (9 Å deep) (*25*).

RESULTS AND DISCUSSION

Quantitative Depth Measurements. To use spin diffusion for quantitative depth measurements, it is important to demonstrate measurement of a known depth reproducibly

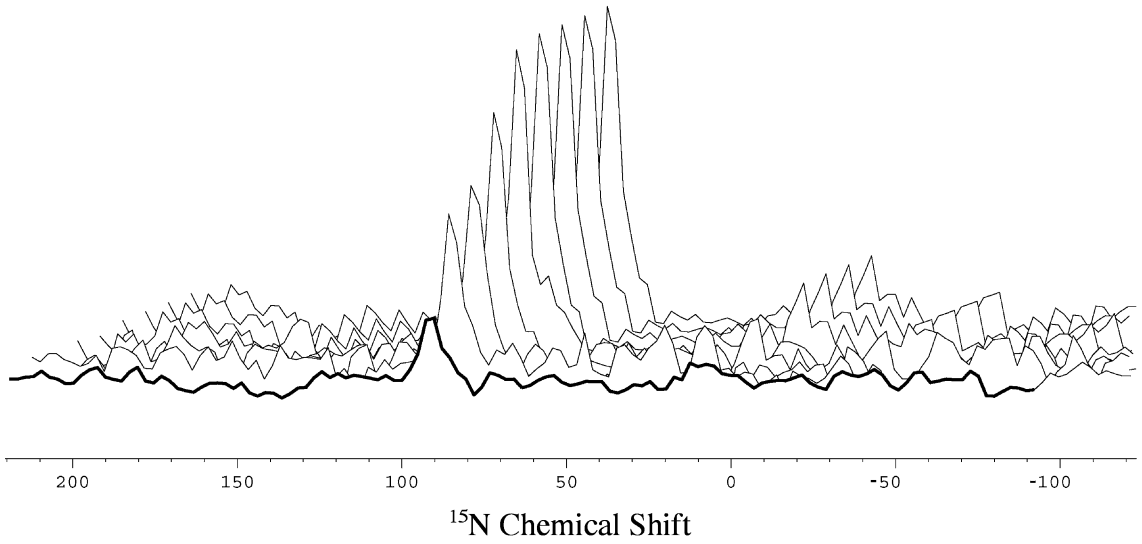

FIGURE 3: ^{15}N spin diffusion spectra of gramicidin A (^{15}N-backbone Trp13 sample) in DMPC bilayers. The spin diffusion times increase from foreground (bold) to background as follows: t_m = 1.0, 1.65, 1.80, 2.69, 3.5, 5.67, 7.24, 8.51, 10.0 ms, with 100 000 scans per spectrum (~28 h each).

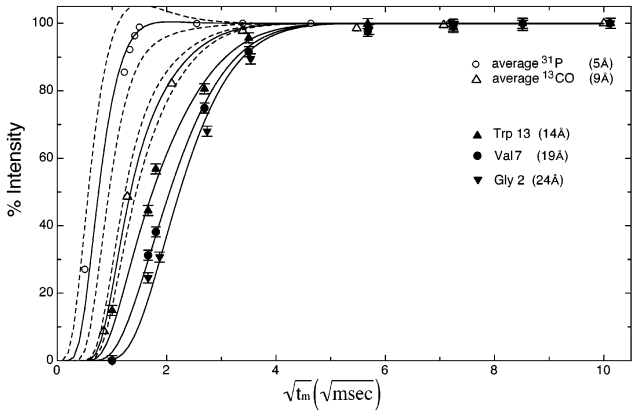

FIGURE 4: ^{31}P, ^{13}C, and ^{15}N spin diffusion profiles for samples of gramicidin A in DMPC bilayers. The spin diffusion data for the lipid ^{31}P (open circles) and carbonyl ^{13}C (open triangles) are the averages of the data for the different gramicidin A samples (lipid data symbol size = error bar size). The depths corresponding to the best-fit simulated curves (solid lines) are given in parentheses. The dashed curves are the ±1 Å curves surrounding the best fit curves (solid lines) for the ^{31}P (5 Å) and carbonyl ^{13}C (9 Å). The ^{15}N spin diffusion data for gramicidin A are shown in filled symbols along with the best fit curves indicating the depths of these residues: Trp13 (filled upright triangles, 14 Å), Val7 (filled circles, 19 Å), Gly2 (filled inverted triangles, 24 Å). Our data are in agreement with the end-to-end dimer depths of these three residues (see Table 2).

Table 2: Depths of Lipid and Gramicidin Sites in the Membrane

	depth			
site	NMR measurement	lipid	end-to-end dimer (1MAG)[a]	double helix (1AV2)[a]
lipid ^{31}P	5 ± 0.5 Å	4 Å		
lipid carbonyl ^{13}C	9 ± 0.5 Å	9 Å		
^{15}N Trp13	14 Å		15.2 Å	16.7 Å
^{15}N Val7	19 Å		20.0 Å	19.1 Å
^{15}N Gly2	24 Å		23.9 Å	9.3 Å
lipid methyl^{13}C	26 ± 2 Å	26 Å		

[a] Depths were deduced from the pdb coordinates as follows. Models were rotated 90° using INSIGHT II to place the membrane normal direction along the *z*-axis. The symmetry of both dimeric structural models makes it possible to deduce the position of the bilayer center: since the plane of symmetry bisecting the membrane normal should correspond to the bilayer center (see Figure 5), the *z*-coordinate for the bilayer center can be deduced by averaging the *z*-coordinates of corresponding residues in each monomer. For instance, the *z*-coordinates of the Gly2 nitrogen in each monomer can be averaged to determine the *z*-coordinate of the bilayer center. Averaging the *z*-coordinates of the Trp13 pair, the Val7 pair, and the Gly2 pair gave the same value for the bilayer center, indicating good alignment with the *z*-axis. The depth of each site was then calculated from the *z*-coordinate of each site by setting the membrane center to a depth of 27.5 Å.

in different samples. The slow step for spin diffusion is the transfer of magnetization from the mobile water protons to the rigid protons of the membrane. Since this rate is likely to vary with temperature and any other factors altering mobility of the water, it might be difficult to compare spin diffusion in different samples. However, experiments comparing spin diffusion for different samples and sample temperatures demonstrate that the line width (full width at half-maximum) of the mobile water proton resonance is a reliable indicator of the overall spin diffusion rate. Figure 2a shows that the ^{1}H spin diffusion profile (the decrease in the mobile water peak due to spin diffusion into the membrane) is reproducible in two different samples when temperatures are chosen to produce 300 Hz line widths for the water in each sample: the data for a gramicidin/DMPC bilayer sample at 245 K (open squares) and a DMPC bilayer sample at 248 K (open circles) are similar. In contrast, when the experiment was performed on the DMPC sample at 245 K (filled squares), it yielded a different proton spin diffusion rate and line width (250 Hz). These results suggest that choosing sample conditions to obtain equivalent proton line widths should yield reproducible spin diffusion to a specific site with a known depth in different samples. This is verified in Figure 2b: the ^{13}C spin diffusion profiles for the carbonyl carbon (increase in the lipid ^{13}C peak) in these samples are indistinguishable for the sample conditions with the same proton line width (open triangles, fit by solid line for 9 Å depth). In contrast, spin diffusion for the DMPC sample at 245 K (filled triangles) would indicate a different depth (8 Å, dashed line). It is reasonable to match the water line width to ensure equivalent spin diffusion rates in different samples,

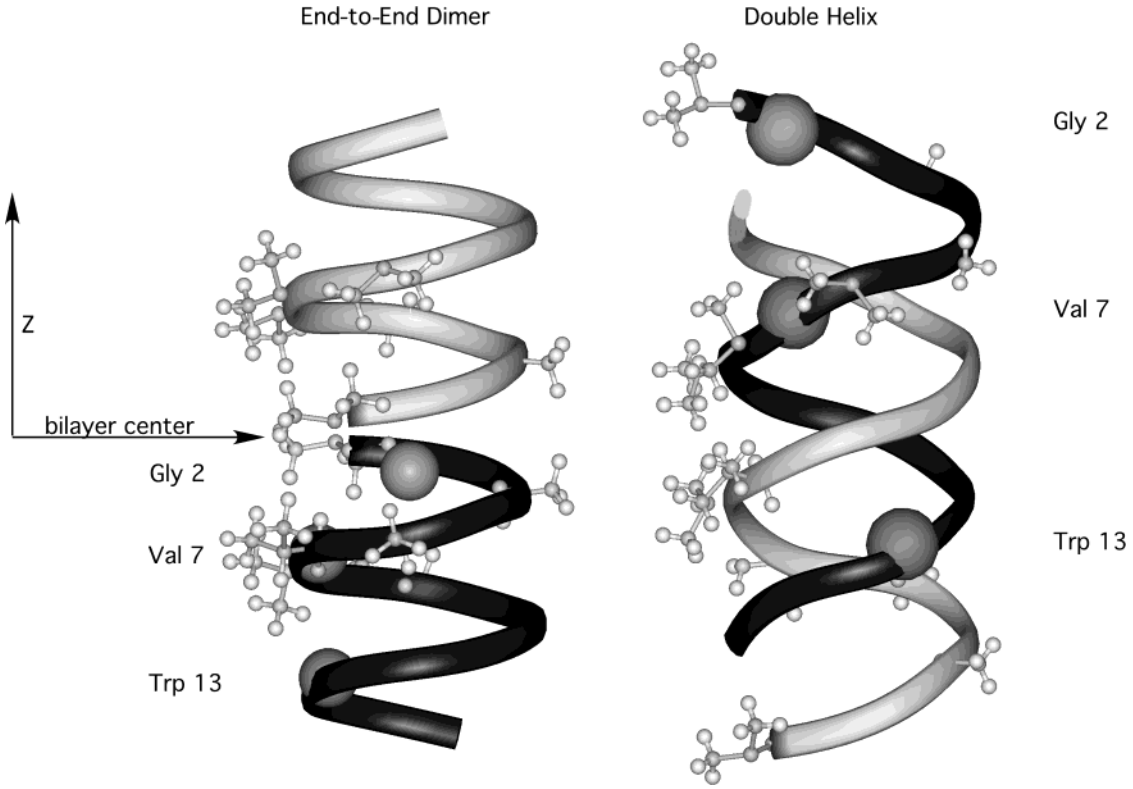

FIGURE 5: Comparison of structural models of gramicidin A. End-to-end dimer (left, PDB code:1MAG) and double helix (right, PDB code:1AV2) models are depicted with a ribbon backbone. Large balls (on one monomer) indicate the positions of the ^{15}N backbone labels (Gly2, Val7, Trp13) that were used for the spin diffusion experiments of Figures 3 and 4. The small ball-and-stick representations (on both monomers) indicate the methyl groups of the side chains of the Val1, Ala3, Ala5, Val6, Val7, Val8 that were probed in the spin diffusion experiments shown in Figures 6 and 7.

since the line width reflects the degree of immobilization of the water and thus the rate of the slow step (transfer from mobile water to immobile protons of the lipid or protein). This slow step must be the same in all samples so that the only differences in overall spin diffusion will be due to the diffusion distance into the membrane, providing a measure of the depth of the sites. Therefore, the line width of the mobile water resonance serves as an internal reference and all spin diffusion experiments described below were performed at temperatures chosen to produce a mobile water line width of 300 Hz.

Our results suggest that sample-to-sample variations should not substantially degrade the precision of the depth measurement. Averaging the spin diffusion data at each mixing time for the lipid ^{31}P in three different samples (data not shown) gave standard deviations of 0.9−2.5%, which is slightly larger than the 0.75% standard deviation of the spectral noise for this strong lipid signal, perhaps due to variations between samples. However, for the weaker signals of sites of interest on a peptide, the standard deviation due to spectral noise will be of comparable magnitude (it is 1.75% for the ^{15}N gramicidin sites in the data presented below), and thus sample variability would increase the error only slightly. For consistency, the error bars used for all data were set to ±1 standard deviation of the spectral noise. At the shallow lipid ^{31}P and ^{13}C sites (4−9 Å), spin diffusion can easily distinguish 1 Å depth differences, suggesting a precision of ±0.5 Å with these strong signals. For the lipid methyl tail (2% error bar), the depth can only be measured to about ±2 Å, due to the much closer spacing of the spin diffusion curves as the depth approaches the center of the membrane. Thus, the precision for spin diffusion measurements of depths of single sites of membrane-bound peptides will typically not be compromised by sample-to-sample variations and will be determined by the signal-to-noise ratio that can be achieved and the depth of the site of interest.

The accuracy of spin diffusion depth measurements is demonstrated using the known depths of the lipid ^{31}P, carbonyl ^{13}C, and methyl ^{13}C. The spin diffusion simulation parameters, specifically the diffusion coefficients, were adjusted to try to simultaneously fit all of these depths. The lipid + peptide diffusion coefficient has the most dramatic effect: even a small adjustment from 37.5 to 40 Å^2/ms changes the depths by 2−3 Å. The water thickness and diffusion coefficient in this phase have little effect: water thicknesses of 12−35 Å and diffusion coefficients of 200−300 Å^2/s gave comparable spin diffusion curves. Parameters were chosen to yield accurate depths (see Table 2) for the lipid carbonyl and methyl carbons but could not precisely match the phosphorus depth (as noted in the previous study (*14*)).

Spin Diffusion Resolves 5 Å Depth Differences. Spin diffusion was performed on ^{15}N-labeled samples of membrane-bound gramicidin A, and results were compared to the known structure in order to demonstrate the resolution capabilities of the technique. Three samples of gramicidin A incorporated into DMPC bilayers, each ^{15}N-labeled at a different backbone position, were used for these experiments. Figure 3 plots a set of ^{15}N spin diffusion spectra (Trp13 sample). Figure 4 plots the spin diffusion profile for each ^{15}N site on gramicidin A and for the lipid ^{31}P and carbonyl ^{13}C measured in the same samples. The data plotted for the lipid ^{31}P are averages

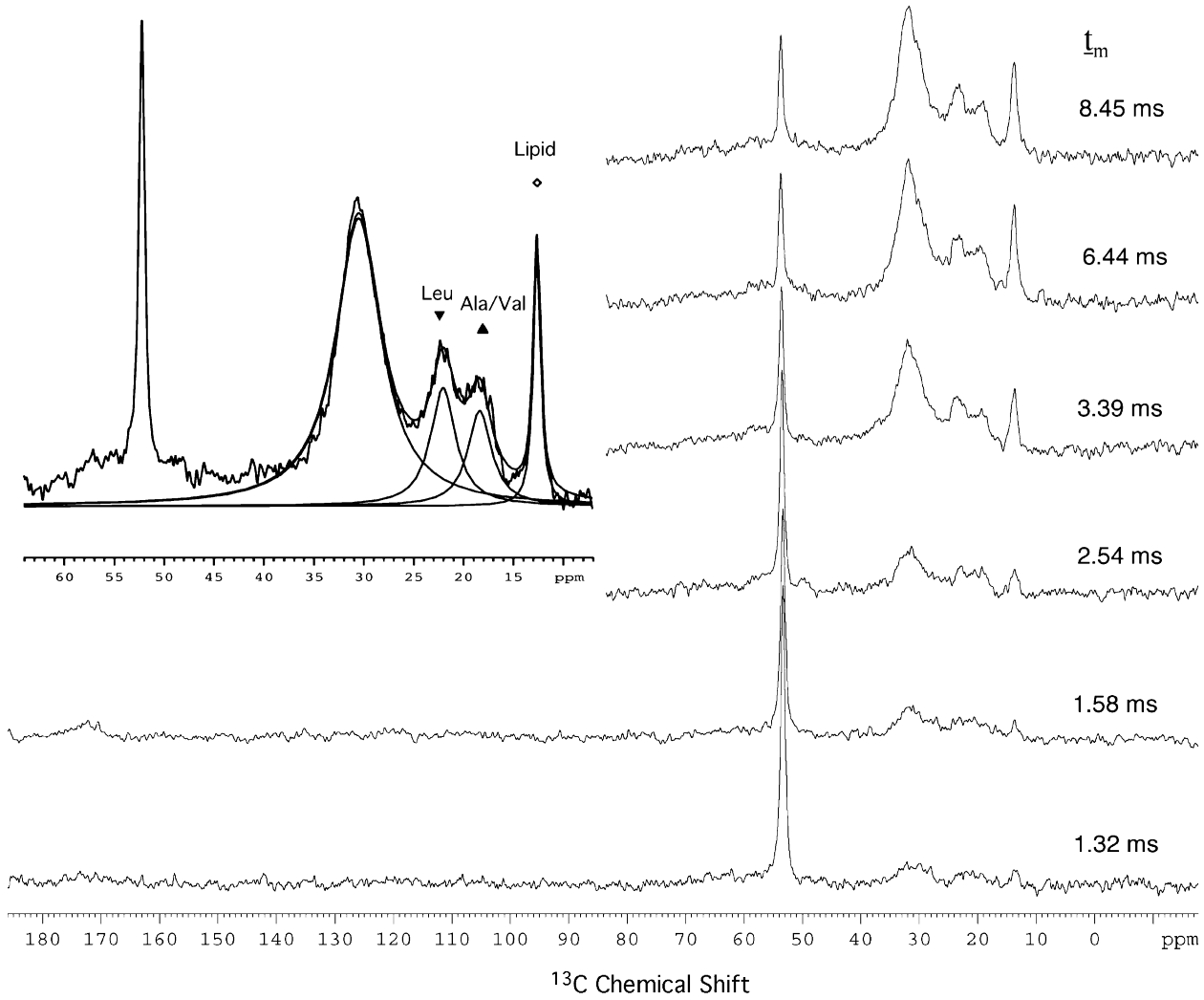

FIGURE 6: Natural abundance ^{13}C spectra of unlabeled gramicidin A in DMPC bilayers. The series of spin diffusion spectra (20 000 scans each) are labeled with the spin diffusion time. The expansion is a CPMAS spectrum (2048 scans) showing the lipid C_γ (55 ppm), CH_2 (28 ppm, predominantly lipid), and the methyl carbon peaks that are assigned to the four Leu residues of gramicidin (22.3 ppm), the six Val and Ala residues of gramicidin (18.6 ppm), and the lipid methyls (12 ppm). Deconvolution of this region of the spectrum was used to analyze spin diffusion spectra to obtain the data plotted in Figure 7, using the symbols shown here above the ^{13}C peaks. The spectra were obtained with an MAS speed of 5 kHz and a sample temperature of 248 K.

of the data for the three samples; the lipid carbonyl ^{13}C data were averaged for only two samples since the Gly2 sample contained 1-^{13}C-Val3 gramicidin A rather than ^{13}C-carbonyl DMPC. The depth of each site is determined by choosing the spin diffusion simulation that best fits the data (curves plotted in Figure 4). The measured depths are summarized in Table 2 and compared to the predicted depths for both the end-to-end dimer structure and the double-helix structure.

The results of these spin diffusion experiments on gramicidin A in DMPC bilayers are in good agreement with the end-to-end dimer structure of gramicidin A in DMPC bilayers (*22*). Figure 5 compares both structural models, with the ^{15}N backbone site labels indicated by large balls. The absolute depth measurements of the backbone nitrogens at positions 7 and 13 do not convincingly discriminate between the two structures, because the depth difference between the two models is only 0.9−1.5 Å at these positions. The measured 24 Å depth of Gly2 clearly fits the end-to-end dimer structure (23.9 Å) and rules out the double-helix structure (9.3 Å). Finally, the 5 Å measured depth differences between successive measured sites is consistent with the end-to-end dimer structure, which has 3.9 and 4.8 Å depth differences, and inconsistent with the double-helix structure, which has 2 and 10 Å depth differences. Thus, the spin diffusion data are incompatible with the double-helix structure, as expected for gramicidin A in DMPC bilayers.

Spin Diffusion on Unlabeled Gramicidin A Distinguishes between Proposed Structures. Spin diffusion experiments on the 1% natural abundance ^{13}C in unlabeled gramicidin A are sufficient to discriminate between the double-helix structure and the end-to-end dimer structure. The methyl resonances in the ^{13}C spectrum of gramicidin A in DMPC vesicles have been assigned on the basis of their ^{13}C chemical shifts (*19*, *26*). Figure 6 shows the ^{13}C natural abundance spectrum with the assignments of the Leu methyl peak (22.3 ppm), the Val/Ala methyl peak (18.6 ppm), and the lipid methyl peak (12 ppm). The depths of the Val and Ala residues (Val1, Ala3, Ala5, Val6, Val7, Val8) within the membrane differ between the two structural models, as shown in Figure 5 (Val and Ala methyls are shown as ball-and-stick representations): these residues are primarily buried in the end-to-end dimer structure (depths of 25.4, 22.9, 21.1, 20.4, 19.5, 18.5 Å, in sequence order) but are found throughout the membrane in the double-helix structure (depths of 9.1, 12.8, 17.7, 20.5,

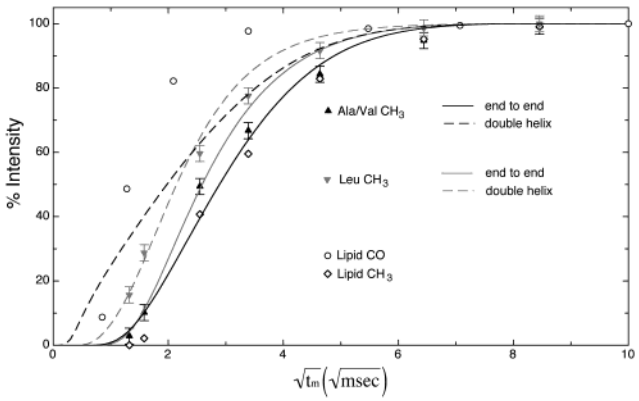

FIGURE 7: Natural abundance ^{13}C spin diffusion profiles for gramicidin A in DMPC bilayers. The lipid carbonyl carbon data (open circles) and lipid methyl carbon data (open diamonds) are plotted for comparison (lipid data symbol size = error bar size). The data and simulations for the methyl of the Val/Ala residues are plotted in black and demonstrate much better agreement with the simulated spin diffusion curve for the end-to-end dimer model (solid black line) than for the double-helix model (dashed black line). The data and simulations for the methyl of the Leu residues are plotted in gray. The closer spacing between the simulations for the end-to-end dimer model (solid gray line) and the double-helix model (dashed gray line) reflect the fact that the depth distribution of the Leu is less distinct than that of Val/Ala in the two structures.

22.8, 23.7 Å). Thus, we expect that spin diffusion data for these methyls could distinguish between the two structures. This is verified by the predicted spin diffusion curves for these sites plotted in black in Figure 7. These curves are calculated by averaging the six spin diffusion curves simulated for each of the depths of the Val/Ala sites. There is clearly a large difference between the solid curve predicted for the buried locations of the Val/Ala in the end-to-end dimer structure and the dashed curve predicted for the more uniform distribution of the Val/Ala in the double-helix structure. The Val/Ala spin diffusion data (black triangles) agree well with the solid black curve for the end-to-end dimer structure. The Val/Ala data also indicate a depth similar to that of the lipid methyl peak (open diamonds), as expected for the buried location of these residues in the end-to-end dimer structure.

The Leu data do not discriminate between the two structural models, because the Leu residues in gramicidin (Leu4, Leu10, Leu12, Leu14) have a similar depth distribution in the end-to-end dimer (average of 16.9 Å for depths of 22.0, 17.1, 15.4, 13.1 Å) and the double helix (average of 15.7 Å for depths of 15.1, 18.5, 16.5, 12.5 Å). The Leu data (gray inverted triangles) fall between the predicted spin diffusion curves for the two structures (gray curves in Figure 7 are averages of curves for the depths of the four Leu sites). In addition to this similar depth distribution, the expected overlap between the Leu resonance and the 23.5 ppm lipid ω-1 carbon resonance also makes it more difficult to use the Leu resonance to distinguish between the structural models of gramicidin A. The comparison between analysis of the Leu and the Val/Ala spin diffusion data illustrates the importance of having a well-resolved peak for which the residues have a very different predicted depth distribution in the two structural models. The Val/Ala spin diffusion data demonstrate that spin diffusion on unlabeled gramicidin A samples can clearly distinguish which of these two structures occurs in lipid bilayers.

Prospects for Spin Diffusion Depth Measurements in Membrane Systems. We have demonstrated that quantitative spin diffusion measurements can be used to characterize the structure of a membrane-bound peptide. In the case of gramicidin A, experiments on the unlabeled peptide are sufficient to distinguish which of two proposed structures occurs in lipid bilayers. The 4−5 Å depth differences measured between successive residues i, $i + 5$, and $i + 11$ in labeled gramicidin A samples are consistent with a β-helix structure inserted perpendicular to the membrane with its N terminus near the bilayer center. Thus, with only three site-specifically labeled samples, spin diffusion measurements on a system of unknown structure would provide insight into the secondary structure, membrane insertion depth and orientation. Furthermore, spin diffusion measurements on unlabeled membrane-bound peptides can, in favorable cases, distinguish between two distinct proposed structures (when the depth distribution of resolved, multiply occurring amino acids differs significantly between the two structures).

Previous work has demonstrated the use of spin diffusion from water (*14*) and from lipids (*13*) to larger membrane proteins (channel-forming colicins) for questions that can be addressed with qualitative measurements of depths of multiple sites. Spin diffusion could in principle provide useful quantitative depth measurements of single sites in membrane proteins in systems where high-precision depth measurements are needed to probe structure or mechanism. However, the low sensitivity of the experiment (the T_2 filter reduces the resonances to about 30% of the intensities in a CPMAS spectrum) would substantially degrade the precision of the depth measurement. Increased sensitivity, achieved using higher field strengths or by observing a more sensitive nucleus such as fluorine in a nativelike *p*-F-Phe side chain, will be needed to make spin diffusion a practical method for precise measurements of depths of single sites in membrane proteins.

Application of spin diffusion to channel-forming peptides or proteins could be complicated by the possibility of mobile water in the channel serving as the source of magnetization so that spin diffusion would no longer correspond to a one-dimensional diffusion from the surface into the membrane. Our results demonstrate that this is not a problem for the gramicidin experiments, most likely because the single file of water in the channel is too small a fraction of the mobile water to be a significant magnetization source. For peptides or proteins forming larger channels or for membrane proteins with large extrinsic domains, there could be significant amounts of mobile water not at the membrane surface. For such membrane proteins, the room-temperature spin diffusion method (*13*) would be advantageous, since the mobile lipid protons in unfrozen samples provide a well-defined source of magnetization for spin diffusion. As previously noted (*13*), this method is less well-suited to membrane-associated peptides because their high mobilities in unfrozen samples results in poor cross-polarization efficiencies.

In summary, spin diffusion from mobile surface water is a good method for characterizing the structure of membrane-associated peptides. Such systems are known to undergo structural changes dependent on solvent, concentration, etc. A disadvantage of spin diffusion is that because high-concentration samples are needed, experiments may not be able to investigate the full concentration range of a concen-

tration-dependent structural change. An advantage is that spin diffusion uses nonperturbing isotopic labels rather than bulky spin or fluorescent labels, which can perturb the conformational equilibria and are too flexible to provide high-resolution depth measurements. Finally, experiments on unlabeled peptides provide a simple means of gaining insight into the membrane-bound structure and discriminating among proposed structural models.

ACKNOWLEDGMENT

We thank Klaus Schmidt-Rohr for providing us with the spin diffusion simulation program, Tim Cross for the isotopically labeled gramicidin samples, Frank Kovacs for help with Insight and MATLAB, and Charlie Dickinson for technical support of the NMR Facility.

REFERENCES

1. Caffrey, M. (2000) A lipid's eye view of membrane protein crystallization in mesophases, *Curr. Opin. Struct. Biol. 10*, 486−97.
2. Rosenbusch, J. P., Lustig, A., Grabo, M., Zulauf, M., and Regenass, M. (2001) Approaches to determining membrane protein structures to high resolution: do selections of subpopulations occur?, *Micron 32*, 75−90.
3. Hunte, C., and Michel, H. (2002) Crystallisation of membrane proteins mediated by antibody fragments, *Curr. Opin. Struct. Biol. 12*, 503−508.
4. Pervushin, K., Riek, R., Wider, G., and Wuthrich, K. (1997) Attenuated T2 relaxation by mutual cancellation of dipole−dipole coupling and chemical shift anisotropy indicates an avenue to NMR structures of very large biological macromolecules in solution, *Proc. Natl Acad. Sci. U.S.A. 94*, 12366−12371.
5. Fanucci, G. E., Cadieux, N., Piedmont, C. A., Kadner, R. J., and Cafiso, D. S. (2002) Structure and dynamics of the beta-barrel of the membrane transporter BtuB by site-directed spin labeling, *Biochemistry 41*, 11543−11551.
6. Hubbell, W. L., Cafiso, D. S., and Altenbach, C. (2000) Identifying conformational changes with site-directed spin labeling, *Nat. Struct. Biol. 7*, 735−739.
7. Pali, T., and Marsh, D. (2002) Structural studies on membrane proteins using non-linear spin label EPR spectroscopy, *Cell Mol Biol Lett 7*, 87−91.
8. Egashira, M., Gorbenko, G., Tanaka, M., Saito, H., Molotkovsky, J., Nakano, M., and Handa, T. (2002) Cholesterol modulates interaction between an amphipathic class A peptide, Ac-18A-NH2, and phosphatidylcholine bilayers, *Biochemistry 41*, 4165−4172.
9. De Foresta, B., Tortech, L., Vincent, M., and Gallay, J. (2002) Location and dynamics of tryptophan in transmembrane alpha-helix peptides: a fluorescence and circular dichroism study, *Eur. Biophys. J. 31*, 185−197.
10. Lavi, A., Weitman, H., Holmes, R. T., Smith, K. M., and Ehrenberg, B. (2002) The depth of porphyrin in a membrane and the membrane's physical properties affect the photosensitizing efficiency, *Biophys. J. 82*, 2101−2110.
11. Thompson, L. K. (2002) Solid-state NMR studies of the structure and mechanisms of proteins, *Curr. Opin. Struct. Biol. 12*, 661−669.
12. Marassi, F. M., and Opella, S. J. (1998) NMR structural studies of membrane proteins, *Curr. Opin. Struct. Biol. 8*, 640−648.
13. Huster, D., Yao, X., and Hong, M. (2002) Membrane protein topology probed by ^{1}H spin diffusion from lipids using solid-state NMR spectroscopy, *J. Am. Chem. Soc. 124*, 874−883.
14. Kumashiro, K. K., Schmidt-Rohr, K., Murphy, O. J., Ouellette, K. L., Cramer, W. A., and Thompson, L. K. (1998) A novel tool for probing membrane protein structure: Solid-state NMR with proton spin diffusion and X-nucleus detection, *J. Am. Chem. Soc. 120*, 5043−5051.
15. Schmidt-Rohr, K., Clauss, J., Blümich, B., and Speiss, H. W. (1990) Miscibility of Polymer Blends Investigated by ^{1}H Spin Diffusion and ^{13}C NMR Detection, *Magn. Res. Chem. 28*, S3−S9.
16. Parker, M. W., Postma, J. P., Pattus, F., Tucker, A. D., and Tsernoglou, D. (1992) Refined structure of the pore-forming domain of colicin A at 2.4 Å resolution, *J. Mol. Biol. 224*, 639−657.
17. Ketchem, R. R., Hu, W., and Cross, T. A. (1993) High-resolution conformation of gramicidin A in a lipid bilayer by solid-state NMR, *Science 261*, 1457−1460.
18. LoGrasso, P. V., Moll, F., III, and Cross, T. A. (1988) Solvent history dependence of gramicidin A conformations in hydrated lipid bilayers, *Biophys. J. 54*, 259−267.
19. Hawkes, G. E., Lian, L. Y., Randall, E. W., Sales, K. D., and Curzon, E. H. (1987) The conformation of gramicidin A in dimethylsulphoxide solution. A full analysis of the one- and two-dimensional ^{1}H, ^{13}C, and ^{15}N nuclear magnetic resonance spectra, *Eur. J. Biochem. 166*, 437−445.
20. Wallace, B. A. (1986) Structure of gramicidin A, *Biophys. J. 49*, 295−306.
21. Wallace, B. A., and Ravikumar, K. (1988) The gramicidin pore: crystal structure of a cesium complex, *Science 241*, 182−187.
22. Ketchem, R., Roux, B., and Cross, T. (1997) High-resolution polypeptide structure in a lamellar phase lipid environment from solid-state NMR derived orientational constraints, *Structure 5*, 1655−1669.
23. Ketchem, R. R., Lee, K. C., Huo, S., and Cross, T. A. (1996) Macromolecular structural elucidation with solid-state NMR-derived orientational constraints, *J. Biomol. NMR 8*, 1−14.
24. Aliev, A. E., and Harris, K. D. M. (1994) Simple Technique for Temperature Calibration of a MAS Probe for Solid-State NMR-Spectroscopy, *Magn. Res. Chem. 32*, 366−369.
25. Buldt, G., Gally, H. U., Seelig, A., Seelig, J., and Zaccai, G. (1978) Neutron diffraction studies on selectively deuterated phospholipid bilayers, *Nature 271*, 182−184.
26. Quist, P. O. (1998) ^{13}C solid-state NMR of gramicidin A in a lipid membrane, *Biophys. J. 75*, 2478−2488.

BI0356101